Metabolomics: Open Access
ISSN: 2153-0769

Kutzner et al., Metabolomics 2014, 4:1
DOI: 10.4172/2153-0769.1000129

Research Article Open Access

Profiling of Terpene Metabolism in $^{13}CO_2$-Labelled *Thymus transcaucasicus*

Kutzner E[1#], Manukyan A[2#] and Eisenreich W[1*]

[1]*Lehrstuhl für Biochemie, Technische Universität München, Lichtenbergstraße 4, 85748 Garching, Germany*
[2]*Center of Life and Food Sciences Weihenstephan, Technische Universität München, Dürnast 4, 85350, Freising-Weihenstephan, Germany*
[#]*Both authors contributed equally to the paper*

Abstract

Metabolism is characterized by the functional pathways and fluxes connecting substrates, intermediates and products of a given organism. Pathways in carbon metabolism can be identified by incorporating ^{13}C-labelled tracers. In the present model study, we have evaluated potential benefits from a single $^{13}CO_2$ pulse-chase experiment with the Caucasian endemic plant *Thymus transcaucasicus* for the analysis of terpene composition and biosynthesis. The study design was conducive of low ^{13}C-enrichments (< 1%) in terpenes that were detected at enhanced NMR-sensitivities without hampering GC-MS-based methods for terpene profiling. From the specific ^{13}C-labelling patterns, pathways of terpene biosynthesis could be gleaned as exemplified for the monoterpene thymol which is made via the non-mevalonate route under the physiological in vivo conditions of the $^{13}CO_2$ experiment.

Keywords: Transcaucasian thyme; *Thymus transcaucasicus*; Lamiaceae; Biosynthesis; Pathway; $^{13}CO_2$; Terpene

Introduction

Non-targeted or semi-targeted metabolite profiling has become a powerful method to determine the composition of small molecules in plant extracts using apolar or polar solvents. In principle, metabolite profiles are specific snapshots (fingerprints) of the metabolic processes that have occurred in the plant under study. Using the tools of GC-MS, LC-MS or ^1H-NMR spectroscopy, crude mixtures can be analyzed to provide information about metabolic profiles. Depending on the specific method, dozens to hundreds (by ^1H-NMR) or hundreds to thousands (by GC-MS or LC-MS) of metabolites can be detected and assigned in a single run [1,2]. Whereas some of these methods (e.g. GC-MS) typically need chemical transformation of the compounds under study, others (e.g. ^1H-NMR) are qualified to deal with the crude mixtures without any prior chemical treatment. On the other hand, the ^1H-NMR approach is hampered by low sensitivity in comparison to MS-based methods, as well as by limited resolution due to the narrow chemical shift range of ^1H-frequencies (i.e. approximately 10 ppm). Due to the even lower sensitivity of ^{13}C-NMR as compared to ^1H-NMR, ^{13}C-profiling is not established in metabolomics, although the ^{13}C-NMR chemical shift range is much larger (i.e. about 200 ppm) than in ^1H-NMR and therefore less compromised by signal overlap. Only recently, ^{13}C-NMR has been introduced as a tool for metabolomics, particularly for the analysis of $^{13}CO_2$-grown photosynthetic bacteria [3]. Using special growth chambers, $^{13}CO_2$-labelling experiments with intact plants revealed considerable details about metabolic pathways under physiological conditions [4-10]. However, all of these studies have not addressed the possibility to combine benefits of ^{13}C-labelling for pathway analysis and ^{13}C-based metabolite profiling from a single experiment. Therefore, we have now performed a model study with $^{13}CO_2$-labelled Transcaucasian thyme (*Thymus transcaucasicus Ronn.*) (Lamiaceae) to assess both metabolite profiles (e.g. isoprenoids) as well as metabolic pathways from the same experiment. This Caucasian endemic species was selected since it is known as a rich producer of essential oils including terpenes [11-13].

Indeed, terpenes (e.g. monoterpenes) constitute the major fraction of secondary metabolites in all thyme species. Generally, terpenes are derived from the basic building units, isopentenyl diphosphate (IPP) and dimethylallyl diphosphate (DMAPP). In all plants, IPP and DMAPP can be synthesized by the well-known mevalonate pathway in the cytosolic compartment of the cell or by the more recently discovered MEP pathway that is operative in the plastids (Figure 1A). Depending on the specific compartment where the final terpene is made, the respective pathway leads to the product. Typically, mono- and diterpenes originate from the plastids and are therefore derived from the MEP pathway (for reviews, see [14-17]). However, mixed biosynthetic patterns were also reported for certain plant terpenes [17-20].

Until now, there is no information available on monoterpene biosynthesis in endemic Thymus species, like *T. transcaucasicus*, while it is established knowledge that thymol from common thyme (*T. vulgaris*) is biosynthesized by aromatization of γ-terpinene to p-cymene followed by hydroxylation of p-cymene [21] (Figure 1B). More recently, it was also reported for cut shoots of *T. vulgaris* that the two isoprene units of thymol are made via the MEP pathway [22]. However, the experimental design of the former study [22] does not rule out effects on the metabolic network due to wounding or the usage of artificial carbon substrates which were used as ^{13}C-labelled tracers in the earlier experiment. In sharp contrast, these intrinsic drawbacks can be avoided by the experimental design of the current study using intact plants and the natural carbon substrate CO_2 as tracer.

Methods

Plant material and study design

A one year old full blooming plant of *T. transcaucasicus* from

***Corresponding author:** Eisenreich W, Lehrstuhl für Biochemie, Technische Universität München, Lichtenbergstraße 4, 85748 Garching, Germany, Tel: +49 89 28913336; Fax: +49 89 28913363; E-mail: wolfgang.eisenreich@mytum.de

Received November 18, 2013; **Accepted** January 24, 2014; **Published** January 31, 2014

Citation: Kutzner E, Manukyan A, Eisenreich W (2014) Profiling of Terpene Metabolism in $^{13}CO_2$-Labelled *Thymus transcaucasicus*. Metabolomics 4: 129. doi:10.4172/2153-0769.1000129

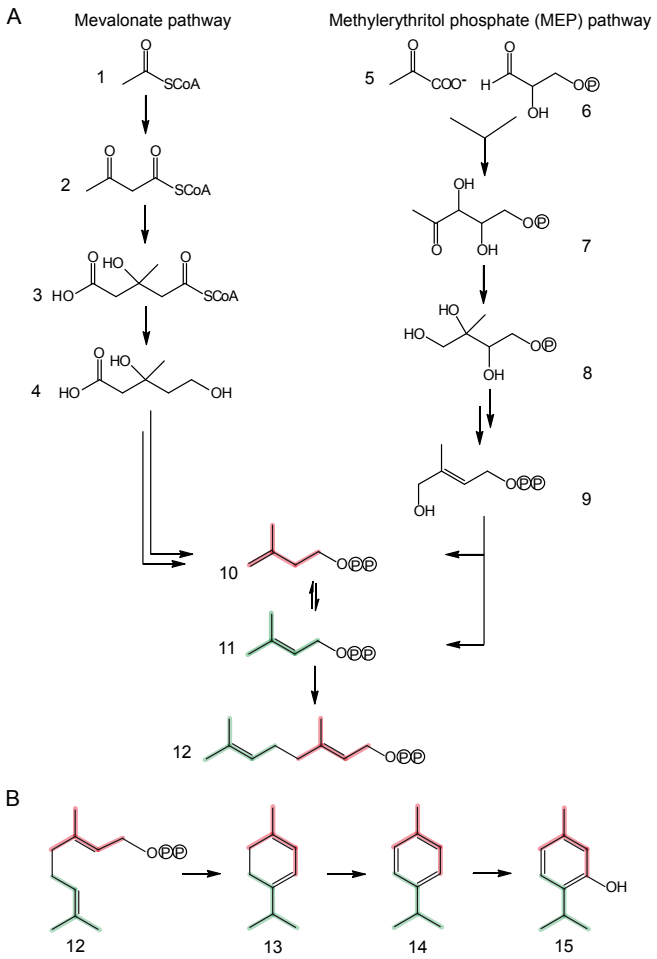

Figure 1: Monoterpene biosynthesis. A. The terpenoid precursors isopentenyl pyrophosphate (IPP, **10**) and dimethylallyl pyrophosphate (DMAPP, **11**) are synthesized in plants via two different pathways, the mevalonate and the methylerythritol phosphate (MEP) pathway. DMAPP (**11**) and IPP (**10**) are further condensed to geranyl pyrophosphate (GPP, **12**) which can be converted into monoterpenes such as thymol (**15**). The isoprene unit derived from IPP (**10**) is highlighted in red, the isoprene unit derived from DMAPP (**11**) in green. **B.** Biosynthesis of thymol (**15**) by aromatization of γ-terpinene (**13**) to *p*-cymene (**14**) followed by hydroxylation of *p*-cymene (**14**).

controlled greenhouse soilless culture was placed into a gas incubation chamber (Advance Optima Biobox AO2000, GWS, Berlin, Germany). The plant was illuminated with white light. The temperature was adjusted to 25°C. Prior to the labelling period with $^{13}CO_2$ (pulse phase), the chamber was flushed with synthetic air (Westfalen AG, Münster, Germany) containing only oxygen (20.5 vol. %) and nitrogen (79.5 vol. %) until the atmospheric unlabelled CO_2 was almost completely removed from the chamber. The plant was then labelled using a mixture of synthetic air and $^{13}CO_2$. The concentration of $^{13}CO_2$ was held constant at 700 ppm by permanently adding the gas from the reservoir (Sigma-Aldrich, Steinheim, Germany) for 4 hours. During this labelling period, the plant consumed about 120 ml of $^{13}CO_2$. Subsequently, the plant was allowed to grow at room temperature under standard greenhouse conditions and under a natural atmosphere (i.e. containing $^{12}CO_2$) for 12 days.

Metabolite profiling: Extraction of terpenes

Terpenes were extracted from the leaves as well as from the flowers of *T. transcaucasicus* with cold chloroform-D ($CDCl_3$) (Sigma-Aldrich, Steinheim, Germany). In more detail, 400 mg of the plant material (fresh weight) were placed into a 10 ml test tube. 2 ml of $CDCl_3$ were added and mixed in an attempt to cover all leaves with the solvent. The mixture was left at room temperature for several minutes. The solvent was then transferred into the next test tube containing another set of 400 mg of plant material from the same plant. These leaves were treated by the same way as the ones in the first test tube. The procedure was repeated again with another portion of 400 mg of fresh material. The solvent was collected and 100 mg of dry $MgSO_4$ were added to remove water. The mixture was held for 30-90 minutes under periodically shaking. Flowers were in general subjected to the same procedure as the leaves. Without further preparation, 200 µl of the extract were used for GC-MS measurements (see below). For NMR analysis, 600 µl of the extract were filled into a 5 mm NMR tube and measured.

Metabolite and isotopologue profiling: Gas chromatography – mass spectrometry

The gas chromatography – mass spectrometry (GC-MS) measurements were performed on a GC 2010 Gas Chromatograph and a GCMS-QP 2010 Plus mass spectrometer coupled to a QP-5000 mass selective detector (Shimadzu, Duisburg, Germany) working with electron impact (EI) ionisation at 70 eV. A Silica capillary column Equity TM-5 (30 m x 0.25 mm x 0.25 µm film thickness) from Supelco Inc. (Bellefonte, PA, USA) was used. An aliquot of the chloroform extract was injected in 1:10 split mode at 230°C and a helium inlet pressure of 82.8 kPa. The interface temperature was 260°C and the helium column flow was 1.17 ml/min. The column was developed at 90°C for 2 minutes and then with a temperature gradient of 5°C/min to a temperature of 150°C followed by a gradient of 50°C/min to a final temperature of 250°C that was held for 2 minutes. Each sample was analyzed three times in order to acquire selected ion monitoring (SIM) data. The identification of the essential oil components was carried out by comparing the retention times and mass data of pure reference compounds, and by comparing data from the NIST05 and NIST05s mass spectral reference library. The relative intensities of the standards and the samples obtained from GC-MS analysis (peak integration) were processed with an in-house Excel-based software package according to [23-26]. This evaluation resulted in the molar ^{13}C-excess of the carbon isotopologues in thymol.

Metabolite and isotopologue profiling: NMR spectroscopy

For the measurement of ^{13}C NMR and INADEQUATE spectra an Avance III 500 system (Bruker, Rheinstetten, Germany) with a cryo probe head (5 mm CPQNP, $^{1}H/^{13}C/^{31}P$/ 19F/29Si; Z-gradient) was used. ^{1}H and ADEQUATE spectra were measured with an Avance I 500 system (Bruker) and an inverse ^{1}H-^{13}C probe head. The resonance frequencies of ^{1}H and ^{13}C were 500.13 MHz and 125.82 MHz, respectively. The temperature was 300 K. The data analysis was done with the MestReNova Software Version 7.0.0 (Mestrelab Research, Santiago de Compostela, Spain). The one-dimensional ^{13}C NMR spectra as well as the one- and two-dimensional spectra ^{1}H NMR spectra were measured with standard Bruker parameter sets.

Results and Discussion

A GC chromatogram of a leave extract from $^{13}CO2$-labelled *T. transcaucasicus* is shown in Figure 2A. About 20 - 30 peaks (> 2% in relation to the highest peak) were detected in typical runs. The

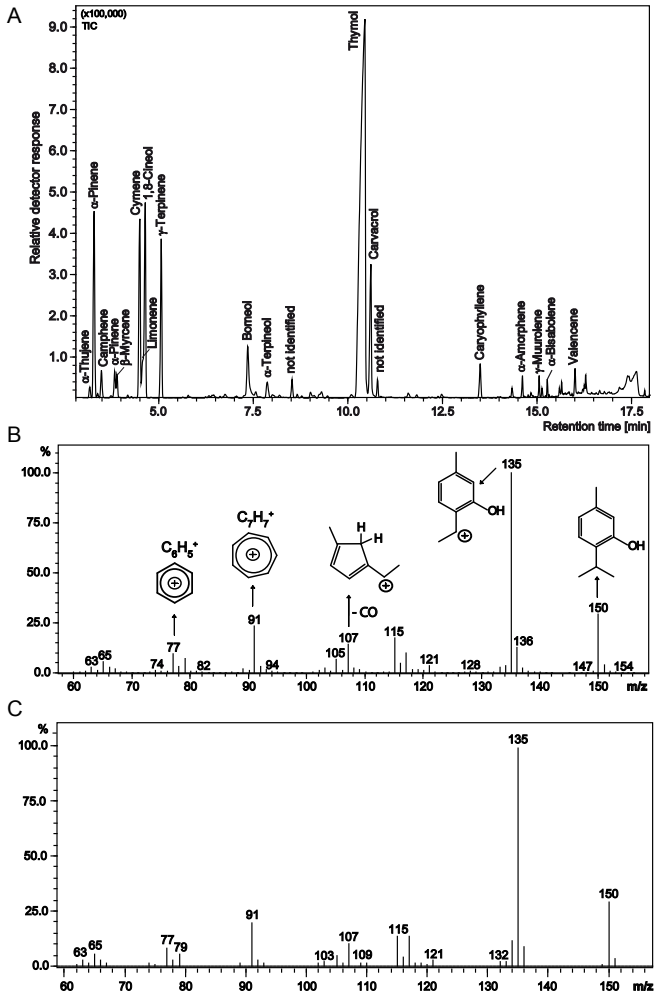

Figure 2: GC-MS analysis of chloroform extract of *T. transcaucasicus* flowers harvested 9 days after the labelling with $^{13}CO_2$ for 4 hours. A. Gas chromatogram performed as described under Experimental. **B.** Corresponding mass spectrum and fragmentation pattern of thymol (molar mass 150.22 g/mol) from the labelled sample. **C.** Corresponding mass spectrum of unlabelled thymol from the NIST05s library.

identification of the essential oil components was performed by comparison with reference data from the NIST05 and NIST05s libraries. It turned out that the weak ^{13}C-enrichments (< 1%) did not disturb the identification of most compounds in the mixture. As a result, the apolar fraction obtained from the leaves as well as from the flowers of *T. transcaucasicus* was predominantly (more than 90% in the overall intensity of all detected peaks) composed of monoterpenes including thymol, γ-terpinene, α-pinene and 1,8-cineol (Figure 3). Sesquiterpenes were only detected at minor amounts, e.g. caryophyllene, germacrene D, α-bisabolene and β-ocimene. In addition to these compounds, the flowers produced additional terpenes, e.g. borneol. These results are in good accordance to previous investigations with *T. transcaucasicus* and other thyme species [12,13,27].

The same chloroform extracts were now also analysed by NMR spectroscopy. A typical ^1H NMR spectrum is shown in Figure 4. Not unexpectedly, the high-field NMR region was crowded due to the presence of multiple compounds in the crude extract. On the other hand, signals in the down-field region were well separated and immediately allowed the assignments of some intense signals to thymol, γ-terpinene, and α-pinene (Figure 4) by comparison with ^1H NMR reference data (own library of ^1H NMR spectra of terpenes (see also Table 1) or data provided by the Spectral Database for Organic Compounds, SDBS). Moreover, the assignments of the signals were confirmed by two-dimensional NMR experiments with the crude mixture (e.g. COSY, HMQC, HMBC) (Table 1 and Figure 5). Notably, the weak ^{13}C-enrichments (< 1%) did not disturb the assignments of the ^1H-NMR signals since the ^{13}C-induced ^1H-satellite signals were small (< 1% in the overall signal intensity of a given ^1H-atom). However, the

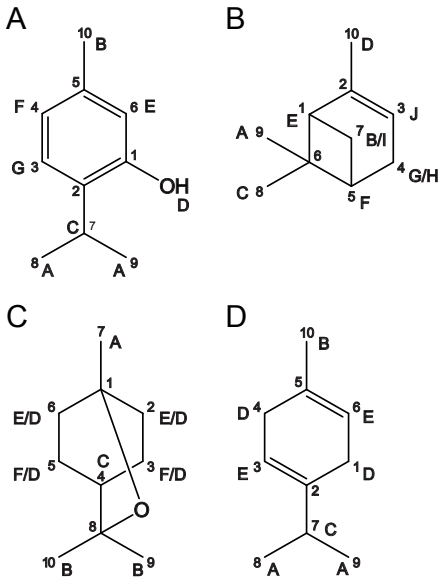

Figure 3: Chemical structures and numbering of the major monoterpenes detected in chloroform extracts of *T. transcaucasicus*. A, thymol. B, α-pinene. C, 1,8-cineole. D, γ-terpinene.

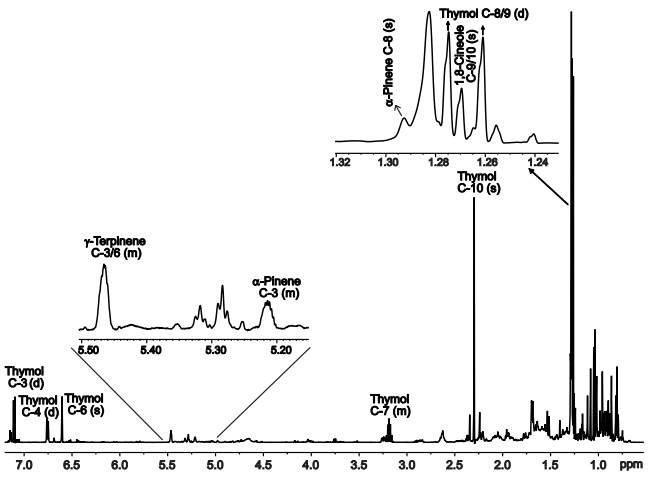

Figure 4: ^1H NMR spectrum of crude leaves extract of *T. transcaucasicus*. Leaves were extracted (see section Experimental) after a chase period of 12 days. The number of scans in the ^1H experiment accounted for 64 and the solvent was $CDCl_3$. The FID was multiplied with a Gaussian function (lb = -1.00; gb = 0.8 Hz).

Compound	^{13}C atom	Chem. Shift δ (ppm)	^{1}H atom	Chem. Shift δ (ppm)		Coupling constant (Hz)		COSY	NOESY[a]	HMBC[a]
Thymol	C-8/9	22.7	A	1.28	(6 H, d)	6.9		C	B, C, G, D(w)	
	C-10	20.9	B	2.31	(3 H, s)			-	A, D, E, F	G(w), C, B(w), A
	C-7	26.7	C	3.20	(1 H, m)	6.9		A	A, D, G	G(w), F, E
	-OH	-	D	4.65	(1 H, s)			-	E, C, B, A(w)	G, E(w), A
	C-6	116.0	E	6.61	(1 H, s)			-	B, D, F, G	-
	C-4	121.7	F	6.77	(1 H, d)	7.9		G	B, E, G	G(w), F, D, B
	C-3	126.2	G	7.12	(1 H, d)	7.7		F	A, C, E, F	G(w), E, B
	C-1	152.5								F(w), D(w), C, B(w)
	C-5	136.7								G, F(w), E(w), D, C, B(w)
	C-2	131.3								G, F(w), E(w), B
										G(w), F, E, D, C, B, A
(+)-α-Pinene	C-9	20.8								
	C-7	31.5	A	0.86	(3 H, s)			-	C, D, E(w), G/H, I, J	
	C-8	26.4	B	1.18	(1 H, d)	8.5		I	C, E(w), F(w), G/H, I, J(w)	B, C
	C-10	23.0	C	1.29	(3 H, s)			-	A, B, D, E, F, G, H, I, J	due to [28]
	C-1	47.0	D	1.68	(3 H, dd)	2.1		-	A, C, E, F, G, H, I, J	A, B, E
	C-5	40.7	E	1.96	(1 H, t)	11.2 1.5		F, I	A(w), B(w), C, D, F(w)	E
	C-4	31.3	F	2.10	(1 H, m)			E, I	B(w), C, D, E(w), G, I(w), J(w)	A, B, C, D, F, I, H(w)
	C-4	31.3	G	2.18	(1 H, m)	17.3	(dd)	H	A, B, C, D, F, H, I, J	A, B, C, E, I, H(w)
	C-7	31.5	H	2.26	(1 H, m)	17.3	(dd)	G	A, B, C, D, G, I, J	due to [28]
	C-3	116.0	I	2.36	(1 H, m)	8.5 11.2		B, E, F	A, B, C, D, F, G, H, J	due to [28]
	C-6	38.0	J	5.21	(1 H, m)			-	A, B, C, D, E, F, G, H, I	due to [28]
	C-2	144.5								-
										A, B, C, E, I, F(w), G(w)
										B, D, E, I, C(w), G(w), H(w)
1,8-Cineole	C-7	27.6								
	C-9/10	28.9	A	1.07	(3 H, s)			-	B, E(w)	
	C-4	32.9	B	1.26	(6 H, s)			-	A, C(w), D(w), F	D(w), E
	C-2/3/5/6	22.8 / 31.5	C	1.42	(1 H, s)			-	B(w), D, E(w), F	B, D(w)
	C-2/6	31.5	D (endo)[b]	1.51	(4 H, m)			E, F	B(w), C, E, F	B, D, E(w), F
	C-3/5	22.8	E (exo)[b]	1.68	(2 H, m)			D, F	D, C(w), F(w)	
	C-1	69.8	F (exo)[b]	2.03	(2 H, m)			D, E	B, C, D, E(w)	A, C, D, E, F
	C-8	73.7								A(w), C(w), D, E, F
										A, D(w), E, F
										B, D, E(w), F(w)
γ-Terpinene[c]	C-8/9	1.0								
	C-10	23.0	A	1.01						
	C-7	34.6	B	1.66						
	C-1/4	31.7	C	2.20						
	C-3/6	118.9	D	2.60						
	C-2	140.6	E	5.43						
	C-5	131.3								

[a]'(w)' indicates a weak correlation signal
[b]due to [29]
[c]all data due to Spectral Database for Organic Compounds SDBS (SDBS No. 23242HSP-06-383)

Table 1: NMR signal assignment of main compounds in essential oils of *Thymus transcaucasicus*. The solvent was $CDCl_3$.

^{13}C-enrichments significantly increased the sensitivity of HSQC and HMBC experiments, thus benefitting the quality of these spectra. More than 100 well defined correlation peaks were observed in the full HMBC spectrum of the extract from the $^{13}CO_2$ labelled plant (Figure 6A), whereas ca. 50 peaks were detected in the spectrum from the unlabelled plant (Figure 6B) (using the same amount of plant material and the same NMR parameters). In accordance to the GC-MS data, thymol was again identified by NMR as the most abundant metabolite in the crude extracts of leaves and flowers. The minor terpenes 1,8-cineole, α-pinene and γ-terpinene could also be clearly assigned in the ^{13}C-enriched sample (Table 1 and Figure 4,5), but hardly in the unlabelled isolate. Nevertheless, it should be noted that the NMR sensitivity with the ^{13}C-enriched sample was still lower than the sensitivity of the GC-MS method. As a consequence, we could hardly detect by NMR some minor terpene compounds which were clearly observed by GC-MS. However, a major benefit of ^{13}C-NMR analysis became obvious when analyzing the metabolic processes leading to terpenes.

As a model compound for pathway analysis, we have selected thymol as the most prominent terpene in the chloroform extract of *T. transcaucasicus*. We have started with a concise analysis of the isotope pattern detected in the MS spectrum of the $^{13}CO_2$-labelled compound.

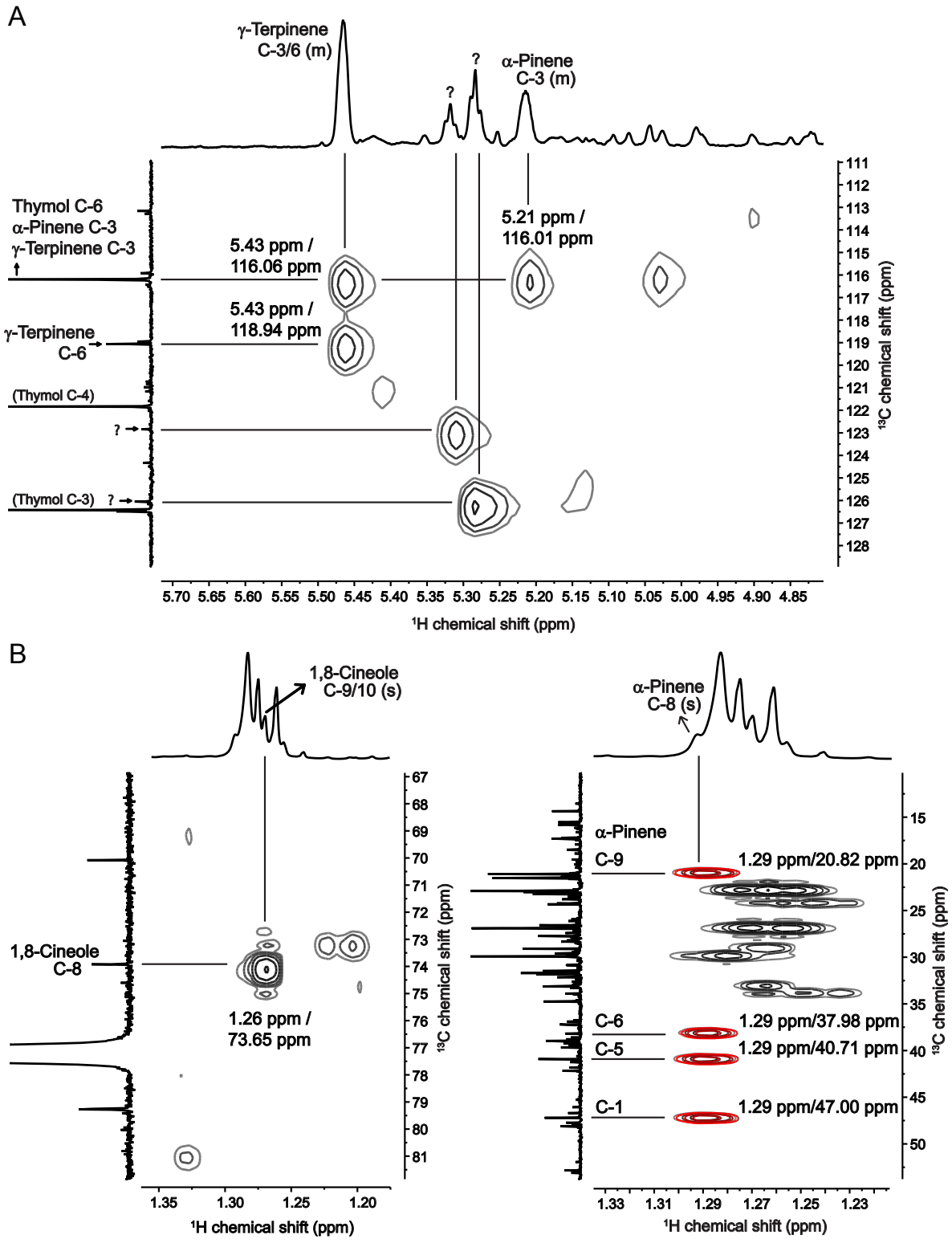

Figure 5: Expanded view of HSQC (A) and HMBC (B) spectra of crude leaves extract of *T. transcaucasicus*. Leaves were extracted (see section Experimental) after a chase period of 12 days. The number of scans accounted for 8 and 16, respectively. The solvent was $CDCl_3$.

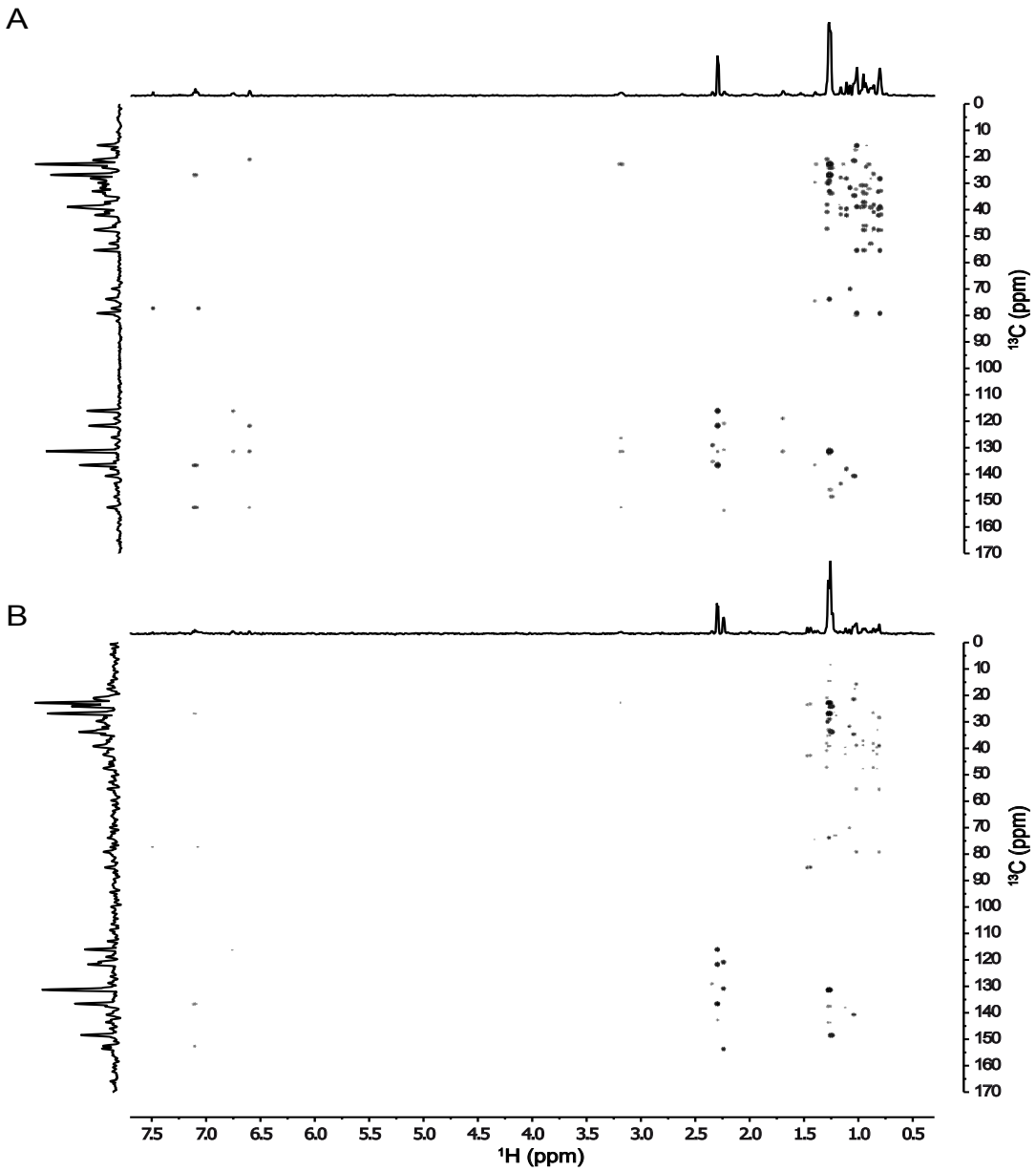

Figure 6: Two-dimensional HMBC spectra of crude leaves extracts of *T. transcaucasicus*. A. Leaves (1.7 g) of the $^{13}CO_2$-labelled plant (4 hour pulse period) harvested after a chase period of 12 days. **B.** Leaves (1.7 g) of an unlabelled *T. transcaucasicus* plant (same developmental stage as the labelled plant). Both spectra were measured with the same standard parameter sets and 16 scans per increment.

The mass spectrum is shown in Figure 2B with a peak at m/z = 150 reflecting the molar mass of thymol. The peaks at m/z = 151, 152, 153, etc. are due to thymol molecules carrying one, two, three, etc. ^{13}C-atoms, respectively. By comparison of the mass intensities with the corresponding ones of a thymol sample at natural ^{13}C-abundance, the ^{13}C-excess values of each isotopologue due to incorporation of $^{13}CO_2$ were calculated. The normalized ratios are displayed in Figure 7. It turned out that thymol was a complex mixture of isotopologues with M+1, M+2, M+3, and M+4 as the most prominent specimens. Isotopologues with more than four ^{13}C-atoms were less abundant (< 20% in all ^{13}C-isotopologues).

Tentatively, isotopologues in thymol comprising three ^{13}C atoms (M+3) can be explained by the MEP pathway which contributes three ^{13}C atoms to the terpene precursors, IPP and DMAPP, via ^{13}C-3 labelled GAP (Figure 8). In contrast, the mevalonate pathway can only contribute two ^{13}C atoms to a given isoprene precursor via the two-carbon moiety in acetyl-CoA. Nevertheless, one has to take into consideration that M+2 isotopologues not only originate from the MVA pathway (starting from acetyl-CoA) but are also transferred to IPP/DMAPP via the pyruvate building block in the MEP pathway (one carbon of pyruvate is lost as CO_2 during the biosynthetic pathway). One also has to take into account that the GAP precursor in the MEP pathway is probably not only $^{13}C_3$ labelled, but also carries a substantial amount of ^{13}C-2 labelled isotopologues that subsequently result in additional

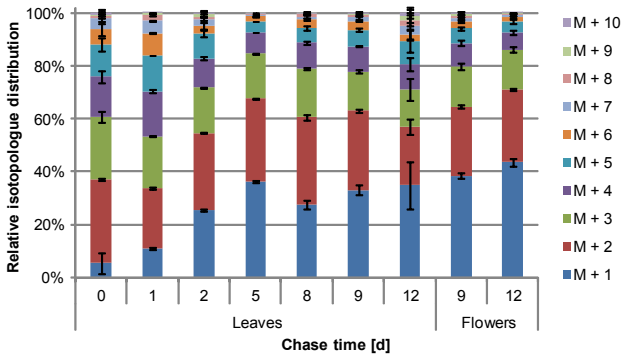

Figure 7: Relative isotopologue distribution (excess) of thymol analyzed by GC-MS. Thymol was extracted with chloroform from *T. transcaucasicus* leaves and flowers at different points of time after the labelling with $^{13}CO_2$ for 4 hours (see Experimental). Excess values were obtained by subtracting the natural ^{13}C abundance of 1.11%. The M+1 bar in the diagram represents molecules carrying only one ^{13}C atom (position unknown), the M+2 bar stands for molecules carrying two ^{13}C atoms, and so on.

M+2 isotopologues of thymol via the MEP pathway. Therefore, it is not possible to assess the absolute rates of thymol formation via the MEP and/or the mevalonate pathway on the basis of these MS data only. Another weakness of the GC-MS thymol data is the lack of positional label information. Unfortunately, the smaller fragments detected in the MS spectrum of the monoterpene are not useful to further elaborate the positional ^{13}C-distribution in the molecule. Nevertheless, the significant amounts of (M+3) isotopologues in the labelled thymol at least suggest its predominant formation via the MEP pathway, as shown earlier for thymol from cut shoots of *T. vulgaris* [22].

In order to further support this hypothesis, the monoterpene was subjected to a detailed NMR analysis. ^{1}H- and ^{13}C-NMR signals of thymol (detected in the chloroform extract, Fig. 9B) could be unequivocally assigned on the basis of literature data and on the basis of two-dimensional experiments (COSY, HSQC, HMBC, ADEQUATE) (Tables 1 and 2) (Figure 9B). For comparison, a ^{13}C-NMR spectrum of an authentic thymol reference is shown in Figure 9A. A closer inspection of the signals of the labelled thymol sample revealed satellite signals due to ^{13}C-^{13}C couplings (Figure 10). To improve the spectral quality, the central and the satellite signals were fitted using the GSD algorithm implemented in the MestReNova software. Mathematically, this module applies a de-convolution of complex spectra transforming them into individual lines. The shape of the lines can further be approximated by using combinations of Lorentzian and Gaussian functions. Whereas for most of the signals sharp satellites were observed due to coupling with one neighboured ^{13}C-atom, the satellite signals of C-1 and C-3 were more complex with an additional fine splitting (8.3 Hz and 2.5 Hz, respectively) indicating the presence of ^{13}C-3-motifs in the molecule. Interestingly, corresponding coupling constants were observed for satellites close to the central signals for C-4 and C-8/9, respectively (see also Table 2 with all detected coupling constants). By comparing these coupling constants, pairs or triples of ^{13}C-atoms in thymol can be assigned as indicated in Table 2. More direct experimental evidence could be provided by ADEQUATE experiments that are based on magnetization transfer via one-bond ^{13}C-^{13}C couplings and a subsequent transfer to the attached proton of the ^{13}C-pair. Due to the specific labelling pattern in the $^{13}CO_2$ labelled thymol samples, only a few (but highly significant) signals were detected in these experiments. As shown in Figure 11B, the 1,1-ADEQUATE experiment displayed signals due to the following transfer paths: ^{13}C-8 → ^{13}C-7 → H-7, ^{13}C-7 → ^{13}C-8 → H-8, ^{13}C-2 → ^{13}C-3 → H-3, ^{13}C-1 → ^{13}C-6 → H-6, ^{13}C-5 → ^{13}C-10 → H-10. This clearly indicates that the biosynthetic process afforded four pairs of directly adjacent ^{13}C-atoms, i.e. 8-7, 1-6, 5-10 and 2-3 (shown in Figure 11B as bars connecting ^{13}C-atoms). Carbon atoms C-4 and C-9 were not incorporated in form of a directly-bound ^{13}C-pair, but only showed long-range ^{13}C-^{13}C couplings (see Figure 10).

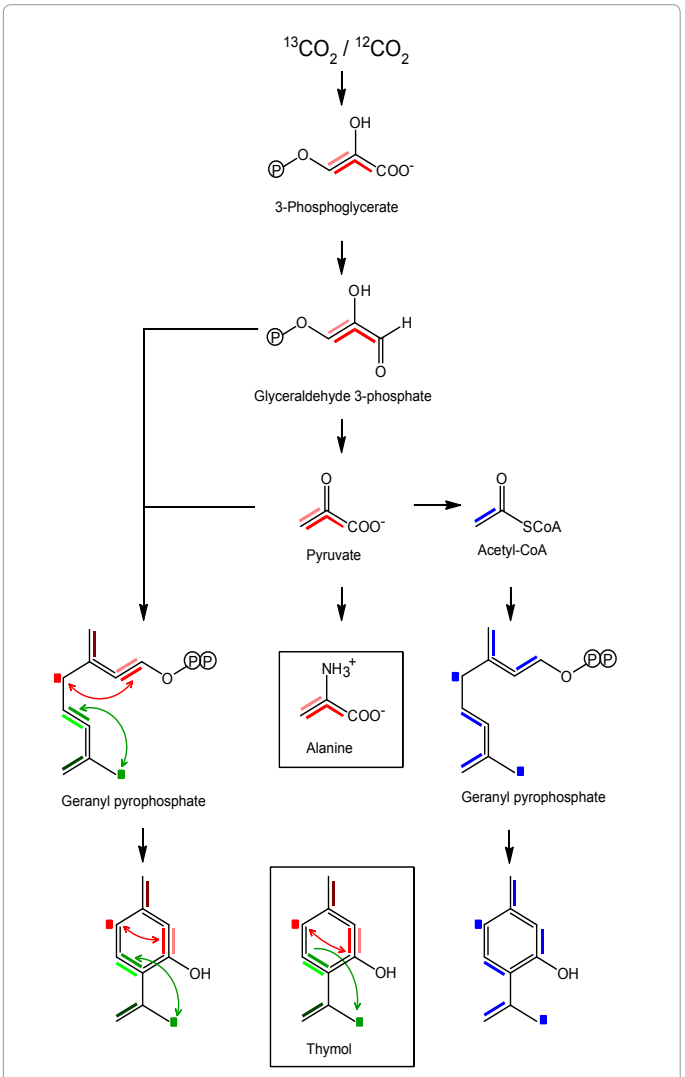

Figure 8: Incorporation of ^{13}C atoms derived from labelling experiments with $^{13}CO_2$ into various metabolites during the plant metabolism. The possible positions of ^{13}C atoms are highlighted as colored bars and small boxes, respectively; the color depends on the metabolic pathway which leads to a certain metabolite. 3-Phosphoglycerate (PGA) and glyceraldehyde 3-phosphate (GAP) are built up in the Calvin cycle which generate either molecules with two ^{13}C atoms (pink bar) or molecules carrying three ^{13}C atoms (red bars). A label at position 1 exclusively is also possible. The synthesis of monoterpenes is possible via the MEP pathway (left side) based on pyruvate and GAP (see Figure 1) which leads to a labelled C_2 block originating from pyruvate (dark red bar and dark green bar, respectively) and/or a C_2 or C_3 block originating from GAP carrying either two ^{13}C atoms (pink and light green bar, respectively) or three ^{13}C atoms (red/green bar and red/green box, respectively), respectively. Red color marks carbon atoms coming from IPP and green color marks carbon atoms coming from DMAPP. On the right side the predicted labelling pattern of thymol arising from the mevalonate pathway based on acetyl-CoA is shown. This path does not generate monoterpenes carrying three ^{13}C atoms. Boxed thymol is displayed with the labelling pattern observed by NMR spectroscopy.

	Chemical shift		Coupling constant[a]		^{13}C enrichment	
Position	^{13}C δ (ppm)		J_{CC} (Hz)		% $^{13}C_{rel.}$ [b]	% $^{13}C^{13}C$ [c]
1	152.50		66.9	(6)	1.10	28.57
			8.3	(4)		
2	131.34		59.9	(3)	1.24	27.01
3	126.23		59.8	(2)	1.12	22.48
			2.5	(9)		
4	121.67		8.4	(1)	1.24	16.67
5	136.66		44.4	(10)	1.17	19.35
6	116.00		66.6	(1)	1.34	21.26
7	26.70		34.6	(8)	1.24	23.66
8/9	22.71		34.5	(7)	1.47	13.79
			2.6	(3)		
10	20.91		44.2	(5)	1.16	22.48

[a]The numbers in parentheses indicate the coupling partners
[b]The signal with the lowest ^{13}C enrichment is referenced to 1.10% ^{13}C
[c]Fraction of the indexed coupling pair in the overall signal intensity of the respective ^{13}C NMR signal

Table 2: ^{13}C-NMR data of thymol obtained from *T. transcaucasicus* flowers labelled with $^{13}CO_2$ for four hours and extracted with chloroform 12 days after the labelling pulse. The solvent was $CDCl_3$.

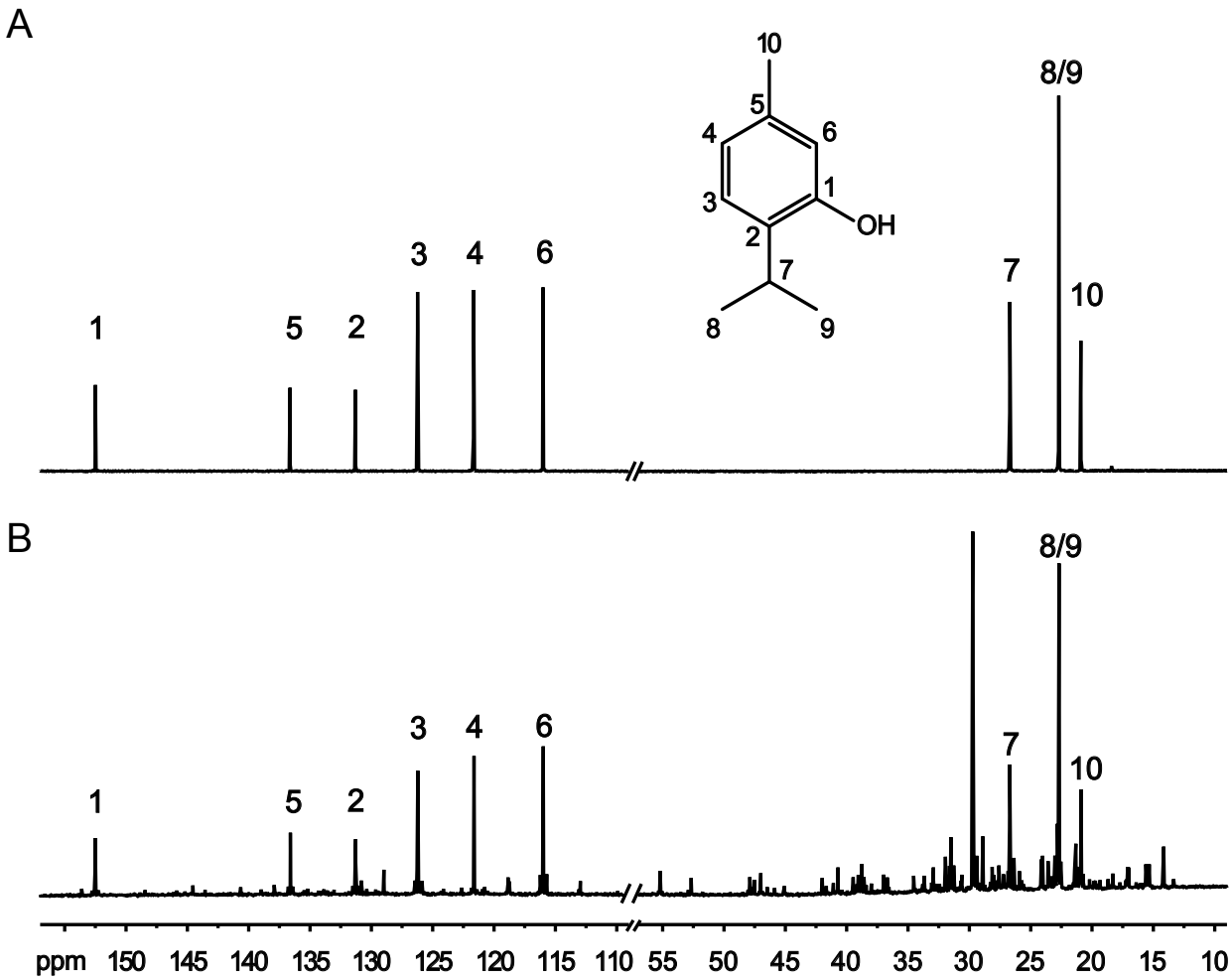

Figure 9: One-dimensional ^{13}C NMR spectra of thymol. A. Standard sample (with natural ^{13}C abundance of 1.1%) of thymol solved in $CDCl_3$. Signals were assigned to the corresponding carbon atoms of thymol. **B.** Sample of *T. transcaucasicus* flowers harvested and extracted with chloroform 12 days after the labelling with $^{13}CO_2$ (4 hours). The solvent was $CDCl_3$.

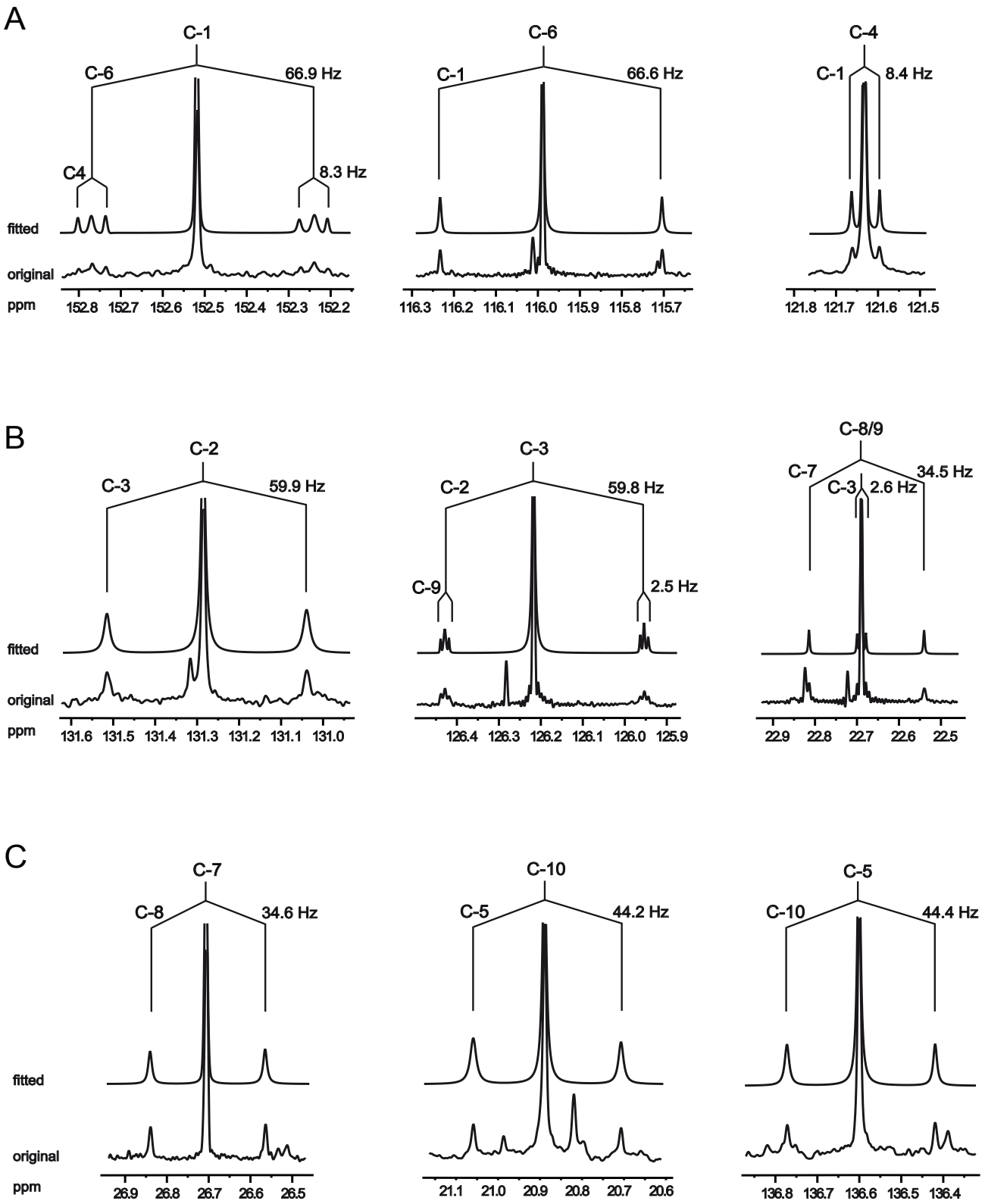

Figure 10: Thymol signals from the one-dimensional ^{13}C NMR spectrum of *T. transcaucasicus* flowers. Flowers were harvested and extracted with chloroform 12 days after the labelling with $^{13}CO_2$ (4 hours). The solvent was $CDCl_3$. The spectrum was processed with MestReNova Software (zero filling 256k). The original spectrum was multiplied by a Gaussian window function of 0.7 Hz except for signals C-8/9 and C-5. For signal C-8/9 and signal C-5 a function of 0.5 Hz and of 1.2 was applied. The numbering of the carbon atoms is displayed in Figure 3.

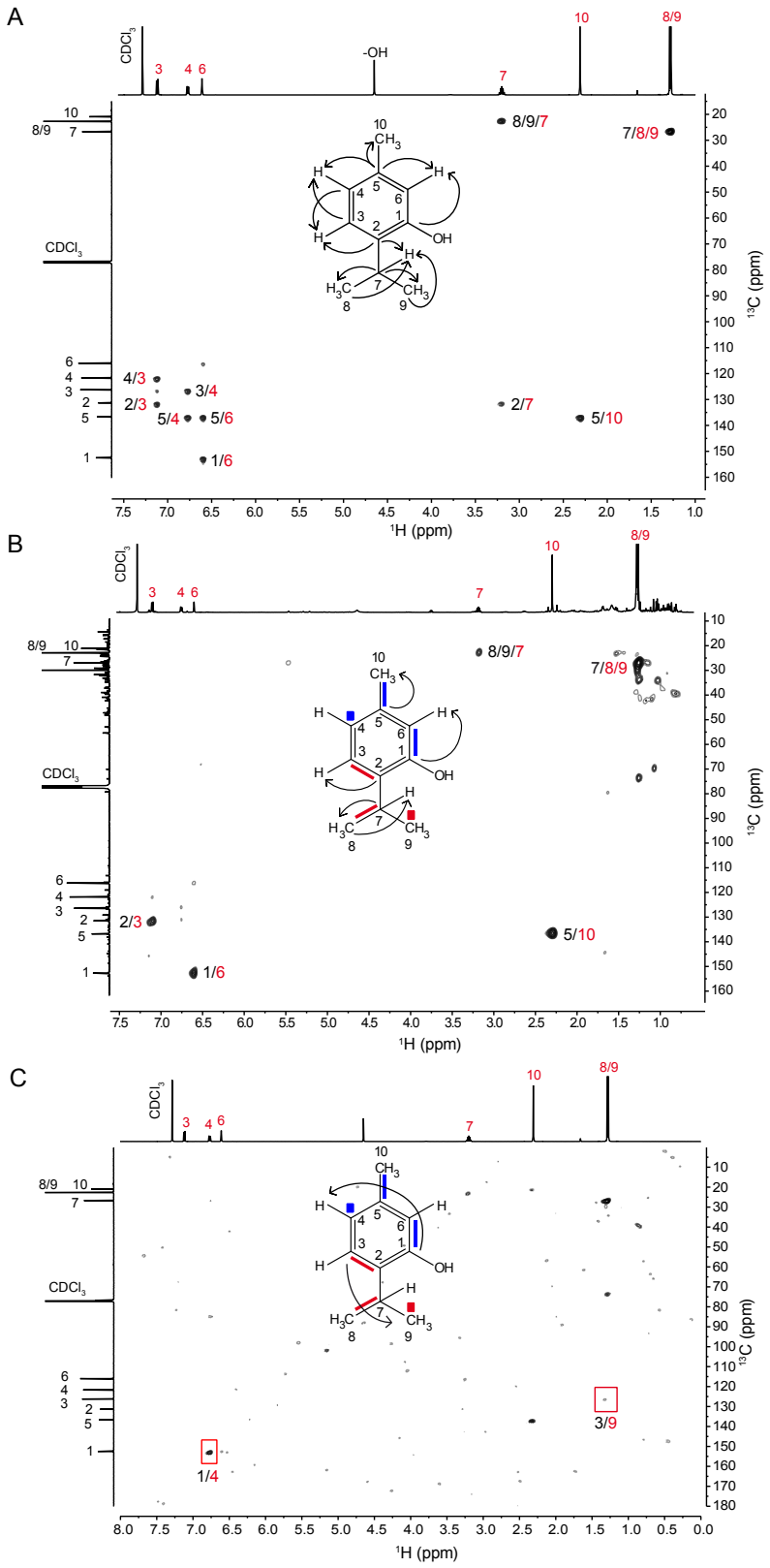

Figure 11: 1,1- and 1,n-ADEQUATE spectra of crude leaves extract of *Thymus transcaucasicus*. A. 1,1-ADEQUATE (65 Hz) of thymol standard solution in $CDCl_3$ (44 mM). **B.** 1,1-ADEQUATE (65 Hz) of crude leaves extract. Leaves were extracted (see section Experimental) after a chase period of 12 days. The solvent was $CDCl_3$. **C.** 1,n-ADEQUATE (8 Hz) of crude leaves extract. Leaves were extracted (see section Experimental) after a chase period of 12 days. The solvent was $CDCl_3$.

Indeed, the expected long-range couplings between C-4 and C-1, and C-9 and C-3, respectively, could be confirmed by 1,n-ADEQUATE experiments which are based on long-range ^{13}C-^{13}C transfer (i.e. via two, or three bonds) followed by direct ^{13}C-^{1}H coupling (i.e. via one bond). As shown in Figure 11C, peaks due to ^{13}C-1 → ^{13}C-4 → H-4 and ^{13}C-3 → ^{13}C-9 → H-9 were observed. These correlations reflected that the carbon atoms 1, 6, 4 and 3, 2, 9 were incorporated as ^{13}C-3-moieties (indicated in Figure 11C as arrows connecting the outlier ^{13}C with a pair of ^{13}C-atoms) during the biosynthetic process. Indeed, these ^{13}C-3 species can be predicted for thymol from ^{13}C-3-labelled GAP via the MEP pathway.

In summary, the NMR-based pathway analysis confirmed that the monoterpene thymol from *T. transcaucasicus* was made predominantly or exclusively via the MEP route of isoprenoid biosynthesis under the physiological conditions of the CO_2 experiment. It should also be emphasized that thymol from the flowers showed the same labelling patterns as that from the leaves. Obviously, thymol was either made in both plant organs via the same pathway or was made in one organ and then rapidly distributed over the whole plant. The labelling pattern also reflected that the linear precursor geranyl diphosphate was converted into the cyclic compound via the known mechanisms of thymol biosynthesis.

Conclusion

The $^{13}CO_2$ pulse-chase experiment was useful for pathway analysis in *T. transcaucasicus*. It should be noted that the experimental method is not restricted to the analysis of terpene metabolism but can also be applied to virtually any metabolic (end)-product found in $^{13}CO_2$-labelled plants as shown by many earlier studies [6-10]. The model study with *T. transcaucasicus* shows that a single $^{13}CO_2$ pulse-chase experiment can not only provide valuable data for pathway analysis, but also can enable ^{13}C-based metabolite profiling at significantly enhanced NMR sensitivity without hampering GC-MS based compound assignment. However, the NMR sensitivity is still lower than in GC-MS analysis, mainly due to the low ^{13}C-enrichments afforded by $^{13}CO_2$ pulse-chase experiments. On this basis, the study design combines benefits of isotope labelling for pathway analysis as well as for metabolite detection. Thus, the experimental settings appear of general value in metabolomics studies with intact plants.

Acknowledgments

We thank the Hans-Fischer-Gesellschaft (München) and the Deutsche Forschungsgemeinschaft (EI 384/8-1) for generous sponsoring of this research work. We also thank the DAAD for supporting A.M.

References

1. Fernie AR, Aharoni A, Willmitzer L, Stitt M, Tohge T, et al. (2011) Recommendations for reporting metabolite data. Plant Cell 23: 2477-2482.
2. Giavalisco P, Köhl K, Hummel J, Seiwert B, Willmitzer L (2009) 13C isotope-labeled metabolomes allowing for improved compound annotation and relative quantification in liquid chromatography-mass spectrometry-based metabolomic research. Anal Chem 81: 6546-6551.
3. Sekiyama Y, Chikayama E, Kikuchi J (2011) Evaluation of a semipolar solvent system as a step toward heteronuclear multidimensional NMR-based metabolomics for 13C-labeled bacteria, plants, and animals. Anal Chem 83: 719-726.
4. Daunicht H, Richter C, Resemann J (1995) An autonomous plant cuvette for advanced climate control and gas exchange measurement. SAE International Technical paper 95, 1536, pp7 ICES, San Diego (CA), Warrendale, PA
5. Krug H, Fink M (1987) Gas-exchange measuring system with adaptive climate control. Biotronics (16):71–74
6. Römisch-Margl W, Schramek N, Radykewicz T, Ettenhuber C, Eylert E, et al. (2007) $^{13}CO_2$ as a universal metabolic tracer in isotopologue perturbation experiments. Phytochemistry 68: 2273-2289.
7. Ostrozhenkova E, Schramek N, Winzenhörlein B, Bacher A, Eisenreich W (2009) Precursor strategies for studies of isoprenoid biosynthesis in plants. In: Palazon J, Cusido RM (eds) Plant secondary terpenoids. Research Signpost, Kerala, pp 75–95
8. Schramek N, Wang H, Römisch-Margl W, Keil B, Radykewicz T, et al. (2010) Artemisinin biosynthesis in growing plants of Artemisia annua. A $^{13}CO_2$ study. Phytochemistry 71: 179-187.
9. Eisenreich W, Huber C, Kutzner E, Knispel N, Schramek N (2013) Isotopologue profiling - towards a better understanding of metabolic pathways. In: Weckwerth W, Kahl G (eds) The handbook of plant metabolomics. Wiley VCH, Weinheim, pp 25–56.
10. Szecowka M, Heise R, Tohge T, Nunes-Nesi A, Vosloh D, et al. (2013) Metabolic fluxes in an illuminated Arabidopsis rosette. Plant Cell 25: 694-714.
11. Kasumov FY, Gadzhieva TG (1982) Components of Thymus transcaucasicus. Chem Nat Compd 18(5):637–638
12. Kasumov F, Komarova V (1983) Essential oils of Thymus transcaucasicusRonn. and Thymus eriophorusRonn. Maslo-Zhir. Prom.-st.:29
13. Manukyan A (2012) Bioactive compounds and their health-promoting capacity of some Caucasian endemic and rare medicinal plants. Acta Hort. (ISHS) (955):339–346.
14. Eisenreich W, Bacher A, Arigoni D, Rohdich F (2004) Biosynthesis of isoprenoids via the non-mevalonate pathway. Cell Mol Life Sci 61: 1401-1426.
15. Gräwert T, Groll M, Rohdich F, Bacher A, Eisenreich W (2011) Biochemistry of the non-mevalonateisoprenoid pathway. Cell Mol Life Sci 68: 3797-3814.
16. Nagegowda DA (2010) Plant volatile terpenoid metabolism: biosynthetic genes, transcriptional regulation and subcellular compartmentation. FEBS Lett 584: 2965-2973.
17. Vranová E, Coman D, Gruissem W (2012) Structure and dynamics of the isoprenoid pathway network. Mol Plant 5: 318-333.
18. Aharoni A, Jongsma MA, Bouwmeester HJ (2005) Volatile science? Metabolic engineering of terpenoids in plants. Trends Plant Sci 10: 594-602.
19. Flügge UI, Gao W (2005) Transport of isoprenoid intermediates across chloroplast envelope membranes. Plant Biol (Stuttg) 7: 91-97.
20. Hemmerlin A, Harwood JL, Bach TJ (2012) A raison d'être for two distinct pathways in the early steps of plant isoprenoid biosynthesis? Prog Lipid Res 51: 95-148.
21. Poulose AJ, Croteau R (1978) Biosynthesis of aromatic monoterpenes: conversion of gamma-terpinene to p-cymene and thymol in Thymus vulgaris L. Arch Biochem Biophys 187: 307-314.
22. Eisenreich W, Sagner S, Zenk MH, Bacher A (1997) Monoterpenoid essential oils are not of mevalonoid origin. Tetrahedron Letters 38(22):3889–3892.
23. Brauman JI (1966) Least squares analysis and simplification of multi-isotope mass spectra. Anal. Chem 38(4):607–610
24. Korzekwa K, Howald WN, Trager WF (1990) The use of Brauman's least squares approach for the quantification of deuterated chlorophenols. Biomed Environ Mass Spectrom 19: 211-217.
25. Lee WN, Byerley LO, Bergner EA, Edmond J (1991) Mass isotopomer analysis: theoretical and practical considerations. Biol Mass Spectrom 20: 451-458.
26. Pickup JF, McPherson K (1976) Theoretical considerations in stable isotope dilution mass spectrometry for organic analysis. Anal Chem 48(13):1885–1890.
27. Stahl-Biskup E (2002) Essential oil chemistry of the genus Thymus - A global view. In: Stahl-Biskup ESF (ed) Medicinal and aromatic plants - Industrial profiles 24 (Thyme), vol. 24. Taylor & Francis, London, pp 75–124.
28. Laihia K, Kolehmainen E, Malkavaara P, Korvola J, Mänttäri P, et al. (1992) 1H, 13C and 17O NMR spectroscopic study of four bicyclo[3.1.1]heptenes (derivatives of a-pinene) and four bicyclo[3.1.1]heptanes (derivatives of ß-pinene). Magn Reson Chem 30(8):754–759.
29. Abraham RJ, Warne MA, Griffiths L (1998) Proton chemical shifts in NMR. Part 12.1 Steric, electric field and conformational effects in acyclic and cyclic ethers. J Chem Soc, Perkin Trans. 2(8):1751–1758.